J|A|C|S COMMUNICATIONS

Published on Web 10/09/2009

Zn−Zn Porphyrin Dimer-Sensitized Solar Cells: Toward 3-D Light Harvesting

Attila J. Mozer,*,† Matthew J. Griffith,† George Tsekouras,† Pawel Wagner,† Gordon G. Wallace,† Shogo Mori,‡ Kenji Sunahara,‡ Masanori Miyashita,‡ John C. Earles,§ Keith C. Gordon,§ Luchao Du,|| Ryuzi Katoh,|| Akihiro Furube,|| and David L. Officer*,†

Intelligent Polymer Research Institute, ARC Centre for Excellence for Electromaterials Science, University of Wollongong, Wollongong 2522, Australia, Department of Fine Materials Engineering, Shinshu University, Nagano, 386-8567, Japan, MacDiarmid Institute for Advanced Materials and Nanotechnology, Department of Chemistry, University of Otago, Dunedin, New Zealand, and National Institute of Advanced Industrial Science and Technology (AIST), Tsukuba Central 5, 1-1-1 Higashi, Japan

Received July 15, 2009; E-mail: davido@uow.edu.au; attila@uow.edu.au

The emulation of the extraordinary photosynthetic light harvesting apparatus has inspired researchers to investigate the assembly and chemistry of a wide variety of covalent and noncovalent porphyrin arrays,[1] but surprisingly there have been very few studies of their use in solar cells.[2] While the enhancement of solar-to-electrical energy conversion efficiency by porphyrin arrays has been theoretically demonstrated,[3] there is little experimental data to support this. In this communication, we demonstrate for the first time that each porphyrin in an array can contribute to current generation in a solar cell.

In the dye-sensitized solar cell (DSSC), light is absorbed by a pigment chemically bound to titanium dioxide, where charge separation occurs.[4] Since the cross section for photon absorption of most pigments is smaller than the geometric area occupied on the surface, light absorption by a pigment monolayer is small.[5] To circumvent this, nanostructured semiconductor electrodes with a surface roughness factor (internal surface area normalized to the geometric area) on the order of a 1000 have been used. Incorporating multichromophore light harvesting arrays with increased absorption cross sections would have the advantage that (i) novel electrode structures with smaller internal surface areas, such as nanotubes,[6] nanowires,[7] or large porosity mesoscopic structures could be used or (ii) efficient DSSCs with thinner dye-sensitized films using ionic liquid[8] or solid state electrolytes could be developed.[9]

The simplest example of a light harvest porphyrin array that could fulfill these requirements is a porphyrin dimer. In 2000, Koehorst et al. reported the first enhanced spectral response of porphyrin dimer-sensitized TiO_2 films.[10] Subsequently, we investigated the use of a variety of porphyrin arrays in DSSCs but did not obtain any evidence for improved photocurrent generation.[11] Here, we have designed new porphyrin dimers, comprising two efficient monoporphyrin dyes linked in either a linear anti (P10) or a 90° syn (P18) fashion, representing simple building blocks of linear or branched 3-D multichromophore arrays. Using femtosecond transient absorption (TA) and absorbed photon-to-current conversion efficiency (APCE) measurements, we show ultrafast, highly efficient electron injection from the photoexcited state of the porphyrin dimers into TiO_2. The results clearly show the contributions of photon absorption by both porphyrin chromophores leading to efficient DSSCs using thin TiO_2 electrodes.

Figure 1 shows the HOMO−LUMO orbitals obtained by DFT calculation for P10 and P18 dimers. DFT calculations show that each porphyrin dimer acts as two noninteracting electronic entities, corresponding to the constituent porphyrin monomers P12 (red and black components of P10 with a COOH linker) and P199 (blue and black components of P18), which we have also synthesized for comparison and are shown in Figure 1S along with the appropriate orbitals. The frontier molecular orbitals of P10 and P18 (Figure 1) are comprised of spatially equivalent P12 and P199 orbitals (Figure S1). The LUMOs of both P10 and P18 correspond to the LUMO of P199, while the HOMOs of both P10 and P18 correspond to the HOMO of P12. Furthermore, the calculated orbital energies for P10 and P18 are largely unperturbed relative to the energies of corresponding monomer orbitals; i.e. they resemble the superposition of the P12 and P199 orbitals (Figures S2 and S3, respectively). This may be due to the 68° dihedral angle between the planes of the two porphyrin monomers within each dimer that inhibits conjugation and electronic communication between the subunits.

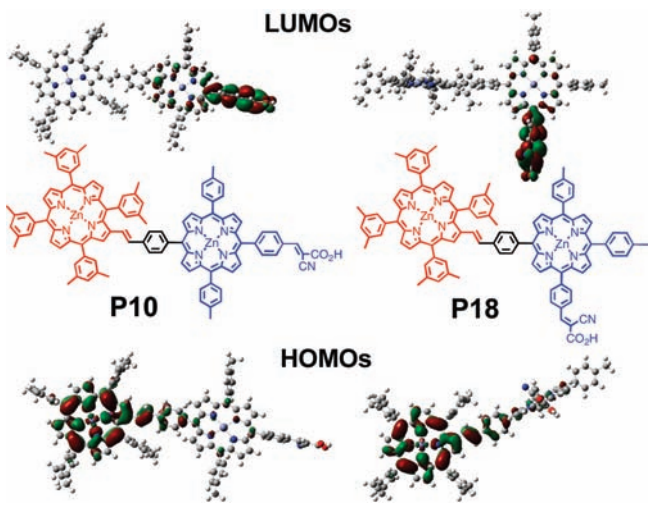

Figure 1. Chemical structures and calculated HOMO/LUMO orbitals (B3LYP/3-21g*) for porphyrin dyes.

In their UV/visible spectra (Figure 2), the dimers show an asymmetrically broadened Soret band and the molar extinction coefficients (ϵ) of their Q-bands are nearly double those of the monomers (Figure 2). Their absorption spectra are a superposition of the monomers and no additional spectral features are observed, indicating negligible interaction between the two porphyrin moieties in the ground state. This is supported by the redox properties investigated by cyclic voltammetry, which show similar oxidation onset potentials (Table S1).

† University of Wollongong.
‡ Shinshu University.
§ University of Otago.
|| AIST.

10.1021/ja9057713 CCC: $40.75

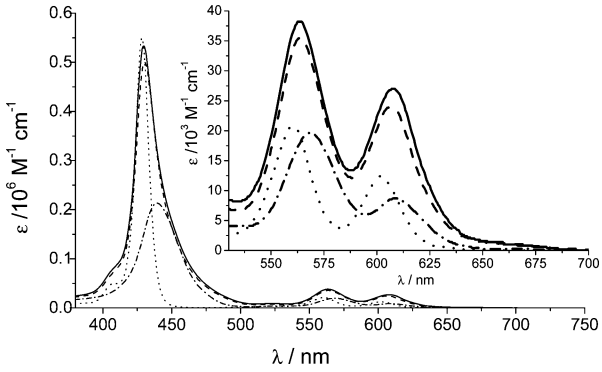

Figure 2. Molar extinction coefficients of P10 (solid line), P18 (dash), P199 (dot), and P12 (dash dot) measured in solution.

Figure 3 shows visible-pump/IR-probe femtosecond transient absorption (TA) signals for TiO_2 films sensitized with P10 porphyrin dimer and bottom monomer P199 in a redox-containing electrolyte (0.1 M lithium iodide LiI, 0.6 M 1,2-dimethyl-3-propylimidazolium iodide DMPImI, 0.5 M 4-*tert*-butylpyridine TBP, and 0.05 M I_2 in acetonitrile). The samples were excited at 532 nm and probed at 3440 nm, with a time-delayed IR probe beam. At 3440 nm photons are primarily absorbed by electrons in the TiO_2 in the absence of dye aggregates.[12] Therefore, electron injection from the photoexcited dye is directly monitored. The TA signals were divided by the absorbed pump intensity $1-10^{-A}$, where A is the absorbance of the dye-sensitized films at the pump wavelength, which allows the comparison of both the injection yield and the injection kinetics. The TA signal was determined for N719 sensitized films in air. The signal maximum of the N719 samples indicated by the red line was taken as 100% injection yield. The risetime of the TA features of the porphyrin-sensitized films is within the time resolution of the setup (250 fs), and no significant difference between the monomer and the dimer can be distinguished. The signal magnitude after 10 ps is similar for both porphyrin dyes, and it is ~70% of the N719-TiO_2 signals. The >50% quantum yield for the porphyrin dimer clearly demonstrates photoinduced electron injection from *both* photoexcited porphyrins within the porphyrin dimers.

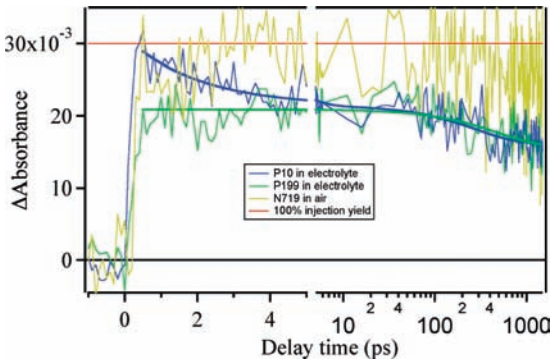

Figure 3. Fs-TA of porphyrin-sensitized TiO_2 films excited by 150 fs pulses at 532 nm and monitored at 3440 nm in the redox containing electrolyte. Signals were divided by the absorbed pump intensity. N719 signals obtained in air are also displayed.

Unlike the N719-TiO_2 signal, the porphyrin-sensitized films show prominent signal decay attributed to electron recombination reaction with the dye cation radical on the 10 ps-to-ns time scale. A ps component of recombination kinetics has been observed in a series of oligo(phenylethylnyl)-linked Zn-porphyrins with a longer binder length and was attributed to electron recombination reactions through space.[13] No difference between the longer dimer and shorter monomer is observed here. There is, however, an additional signal at <10 ps for the dimer. We have measured similarly fast TA signals for porphyrin films on SiO_2 substrates that may be attributed to delocalized excited states in, for example, dye aggregates.

Although O'Regan and Grätzel report a high quantum efficiency for a trimeric ruthenium complex dye in their original *Nature* paper,[4] to the best of our knowledge Figure 3 is the first spectroscopic report of efficient and fast charge injection of photoexcited organic multichromophore units bound to TiO_2.

Table 1. Photovoltaic Parameters and Dye Uptake of Porphyrin Dyes

DYE	J_{sc} [mA cm^{-2}]	V_{oc} [mV]	FF	Eff. [%]	U^a
P10	6.87	700	0.66	3.2	1.2
P18	6.78	710	0.65	3.1	1.2
P199	6.25	670	0.67	2.8	1.5
P12	5.10	620	0.66	2.1	1.2
N719	5.51	750	0.70	2.9	0.9
P10*	8.04	715	0.65	3.8	1.2

[a] Dye uptake $\times$ 10^{-8} mol cm^{-2} μm^{-1}.

To achieve efficient charge injection for the chromophore not directly linked to the electron acceptor, the photoexcitation is either transferred to the first chromophore (by energy or electron transfer)[10] or it may also directly inject an electron. Due to the fast risetime of the signals in Figure 3, we cannot distinguish which mechanism operates. The dye uptake measurements (Table 1) show that the porphyrin monomer and dimers are absorbed onto TiO_2 in similar amounts and near the dye uptake maximum ($(1.2-1.5) \times 10^{-8}$ mol cm^{-2} μm^{-1}) for full surface coverage. This is surprising given that it might appear at first sight that P18 should occupy twice the surface area given its angular conformation. Electron injection and recombination kinetics are quite similar for both P10 and P18 (not shown), which suggests that the constituent porphyrins of each dimer are situated at a comparable distance from the TiO_2 surface. Therefore, we propose that P10 and P18 bind in a similar fashion as illustrated in Figure 4, which accounts for both the similar surface coverage and their near-identical kinetics.

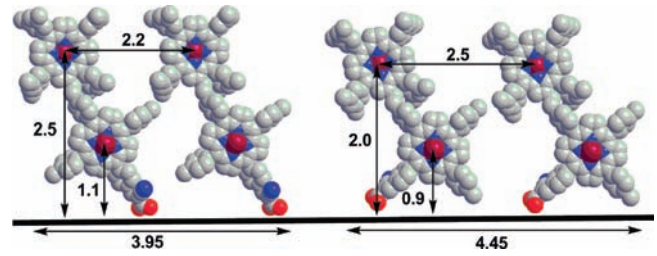

Figure 4. Schematic representation of P10 and P18 dimer arrangement on the TiO_2 surface.

Solar cell efficiencies of DSSCs based on porphyrin-sensitized, transparent 2.5 μm TiO_2 films (Solaronix-T) are shown in Table 1. The short circuit current J_{sc} of both dimers is significantly higher than that of N719 and up to 10% higher than that of the P199 porphyrin dye. We can also say that no major difference between the P10 and P18 dimer is observed under these similar fabrication conditions. As has been observed previously for porphyrin dyes, the open circuit voltage V_{oc} of all the porphyrin DSSCs is lower than that of N719 due to shorter electron lifetimes.[14] However, the V_{oc} of the dimers is improved by up to 80 mV compared to the

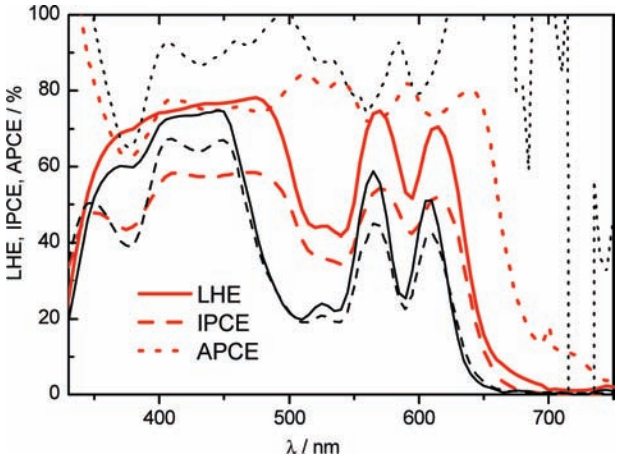

Figure 5. Light harvesting (LHE), incident photon-to-current conversion (IPCE), and absorbed photon-to-current conversion (APCE) efficiency of P10 (red) and P199 (black)-sensitized TiO_2 solar cells.

monoporphyrin dyes. This suggests that the closely packed, bulky porphyrin dimers have a surface blocking effect, preventing the approach of the electron-accepting species of the electrolyte to the TiO_2 interface.

We have observed that the performance of the dimer-sensitized DSSC is highly dependent on the dye uptake conditions. Optimization of the fabrication parameters on a 3 μm thick TiO_2 film have yielded an improved 3.8% P10 DSSC (P10* in Table 1; N719 and P199 was 3.4% and 3.1%, respectively). These results on thinner TiO_2 films (2.5 μm) clearly demonstrate the advantage of multichromophore light harvesting arrays, where doubling the dye absorption coefficient results in significantly improved light harvesting efficiency (LHE), although this will not affect the maximum achieveable efficiency of a fully optimized thick film DSSC, whose efficiency is dominated by the spectral coverage rather than absorption coefficient. It will, however, be beneficial for solid state and quasi-solid state DSSCs or other dye-sensitized photoelectrochemical devices in which the total internal surface area for dye uptake is limited.

The LHE (defined as the fraction of absorbed photons to incident photons on the sample) of the best dimer-sensitized TiO_2 film (P10*) is ~20% higher than that of the P199 monomer due to the similar dye uptake (Table 1) and the much higher molar extinction coefficient (Figure 5) demonstrating the clear advantage of the concept used in these thin devices. The incident photon-to-current conversion efficiency (IPCE) of the dimer, which includes contribution from light harvesting, electron injection, and charge collection, is ~10% larger than that of P199 in the Q-band spectral region. It is above 50%, which can only be achieved if both porphyrin units contribute to charge injection. The absorbed photon-to-current conversion (APCE) efficiency (calculated as IPCE/LHE; see SI) in the absence of charge collection losses (note that thin TiO_2 films were used) is determined by the charge injection efficiency. The APCE values are ~70 − 80% for both P10 and P199, consistent with the TA measurements. The <100% APCE may be attributed to the observed fast component of the recombination kinetics in Figure 3, which clearly competes with the dye cation regeneration process, which has been shown to occur on the ns to μs time scale. The fs-TA spectra as well as the IPCE/APCE measurements independently confirm that both porphyrin chromophores contribute to charge injection.

In conclusion, we have successfully synthesized porphyrin dimers, where both porphyrin component chromophores show efficient electron injection into TiO_2. DFT calculations suggest that the two component porphyrins of each dimer do not significantly interact in their ground state. By incorporating the porphyrin dimers into DSSCs, we have achieved up to 70% APCE. Surprisingly, no major difference in dye uptake, injection efficiency, or device performance has been observed between the linear or angled dimer, suggesting both of these building blocks could, in principle, be used to construct larger 3-D multichromophore light harvesting arrays with efficient solar energy conversion.

Acknowledgment. Financial support from the Australian Research Council, DEST and the MacDiarmid Institute for Advanced Materials and Nanotechnology is gratefully acknowledged.

Supporting Information Available: Synthesis of compounds, UV−visible spectroscopy, cyclic voltammetry, DFT calculations and geometry optimization, dye solar cell fabrication, APCE calculations. This material is available free of charge via the Internet at http://pubs.acs.org.

References

(1) Burrell, A. K.; Officer, D. L.; Plieger, P. G.; Reid, D. C. W. *Chem. Rev.* **2001**, *101*, 2751.
(2) Hasobe, T.; Kashiwagi, Y.; Absalom, M. A.; Sly, J.; Hosomizu, K.; Crossley, M. J.; Imahori, H.; Kamat, P. V.; Fukuzumi, S. *Adv Mater.* **2004**, *16*, 975. Splan, K. E.; Massari, A. M.; Hupp, J. T. *J. Phys. Chem. B* **2004**, *108*, 4111. Imahori, H. *J. Phys. Chem. B* **2004**, *108*, 6130–6143. Hasobe, T.; Kamat, P. V.; Absalom, M. A.; Kashiwagi, Y.; Sly, J.; Crossley, M. J.; Hosomizu, K.; Imahori, H.; Fukuzumi, S. *J. Phys. Chem. B* **2004**, *108*, 12865. Gervaldo, M.; Otero, L.; Milanesio, M. E.; Durantini, E. N.; Silber, J. J.; Sereno, L. E. *Chem. Phys.* **2005**, *312*, 97. Hasobe, T.; Murata, H.; Fukuzumi, S.; Kamat, P. V. *Mol. Cryst. Liq. Cryst.* **2007**, *471*, 39. Dy, J. T.; Tamaki, K.; Sanehira, Y.; Nakazaki, J.; Uchida, S.; Kubo, T.; Segawa, H. *Electrochemistry* **2009**, *77*, 206.
(3) Hasselman, G. M.; Watson, D. F.; Stromberg, J. R.; Bocian, D. F.; Holten, D.; Lindsey, J. S.; Meyer, G. J. *J. Phys. Chem. B* **2006**, *110*, 25430.
(4) O'Regan, B.; Grätzel, M. *Nature* **1991**, *353*, 737. Grätzel, M. *Nature* **2001**, *414*, 338A.
(5) Grätzel, M. *J. Photochem. Photobiol., A* **2004**, *164*, 3.
(6) Martinson, A. B. F.; Elam, J. W.; Hupp, J. T.; Pellin, M. J. *Nano Lett.* **2007**, *8*, 2183.
(7) Mor, G. K.; Shankar, K.; Paulose, M.; Varghese, O. K.; Grimes, C. A. *Nano Lett.* **2006**, *2*, 215.
(8) Kuang, D.; Ito, S.; Wenger, B.; Klein, C.; Moser, J. E.; Humphry-Baker, R.; Zakeeruddin, S. M.; Grätzel, M. *J. Am. Chem. Soc.* **2006**, *128*, 4146.
(9) Bach, U.; Lupo, D.; Comte, P.; Moser, J. E.; Weissörtel, F.; Salbeck, J.; Spreitzer, H.; Grätzel, M. *Nature* **1998**, *395*, 583.
(10) Koehorst, R. B. M.; Boschloo, G. K.; Savenije, T. J.; Goossens, A.; Schaafsma, T. J. *J. Phys. Chem. B* **2000**, *104* (10), 2371.
(11) Campbell, W. M.; Burrell, A. K.; Officer, D. L.; Jolley, K. W. *Coord. Chem. Rev.* **2004**, *248*, 1363–1379.
(12) Furube, A.; Katoh, R.; Hara, K.; Sato, T.; Murata, S.; Arakawa, H.; Tachiya, M. *J. Phys. Chem. B* **2005**, *109*, 16406. Wang, Z.-S.; Koumura, N.; Cui, Y.; Takahashi, M.; Sekiguchi, H.; Mori, A.; Kubo, T.; Furube, A.; Hara, K. *Chem. Mater.* **2008**, *20*, 3993.
(13) Chang, C.-W.; Luo, L.; Chou, C.-K.; Lo, C.-F.; Lin, C.-Y.; Hung, C.-S.; Lee, Y.-P.; Diau, E. W.-G. *J. Phys. Chem. C* **2009**, *113*, 11524–11531.
(14) Mozer, A. J.; Wagner, P.; Officer, D. L.; Wallace, G. G.; Campbell, W. M.; Miyashita, M.; Sunahara, K.; Mori, S. *Chem. Commun.* 2008, 4741.

JA9057713